Rehabilitation of Unreinforced Brick Masonry Walls Using Composites

Mohamed AbdelMonem ElGawady, Pierino Lestuzzi, Marc Badoux
Swiss Federal Institute of Technology at Lausanne EPFL, Switzerland

1 Introduction

Unreinforced masonry (URM) buildings represent a large portion of the buildings around the world. Most of these buildings were built with little or no considerations for seismic design requirements. Recent earthquakes have shown that many such buildings are seismically vulnerable; therefore, the demand for upgrading strategies of these buildings has become increasingly stronger in the last few years. Moreover, based on modern design codes most of the existing URM buildings need to be upgraded. For example, under the URM Building Law of California, passes in 1986, the buildings evaluation showed that approximately 96% of the URM buildings needed to be retrofitted, which would result in approximately $4 billion in retrofit expenditure [5]. In Switzerland, a recent research [13] carried out on a target area in Basel shows that from 45% to 80% of the existing URM buildings, based on construction details, will experience heavy damage or destruction during a moderate earthquake event. Thereby, improving existing and developing better methods of upgrading existing seismically inadequate buildings is an urgent need. Numerous techniques are available to increase the strength and/or ductility of URM walls. There seems to be a reliability issue with some of the commonly used techniques. Modern composite materials offer promising upgrading possibilities for masonry buildings. This paper presents a pioneer dynamic in-plane tests carried out on half-scale unreinforced masonry walls rehabilitated with composites (URM-WUC).The objective of this study is to use dynamic tests to better understand the behavior of URM-WUC subjected to in plane seismic loading and to investigate the effectiveness of composite materials as one side externally bonded rehabilitation materials.

2 Experimental program

Two years ago, two-phases research program on the effectiveness of using composites as rehabilitation material for URM walls have been switched on. The first phase includes testing of slender and squat URM specimens until a predefined degree of damage then strengthening these specimens using different products of fiber reinforced plastics (FRP). The second phase includes static cyclic tests of squat and midget rehabilitated specimens using composites or shotcrete. In the second phase, specimens were tested as URM specimens first until predefined degree of damage (precracked) then strengthened and other specimens were upgraded directly after construction (uncracked). This paper presents the results of the first phase i.e. the dynamic tests.

2.1 Test Specimens

Due to the limitations of the test set-up (size and capacity) half-scale single wythe walls were constructed using half-scale hollow clay masonry units. The test specimens had 2 aspect ratios (Figure 1): slender walls and squat walls; also, two mortar types were used: weak (M2.5) and strong (M9). In addition, different types of FRP (Table 1) and upgrading configuration (Figures 2 and 3) were used to upgrade the specimens. Anchorage failure of the FRP was prevented by clamping the FRP ends to specimen's footing and cap beam using steel plates and screw bolts, (since anchorage problem is out of the scope of this research). Both the cap beam and footing pad were pre-cast reinforced concrete.

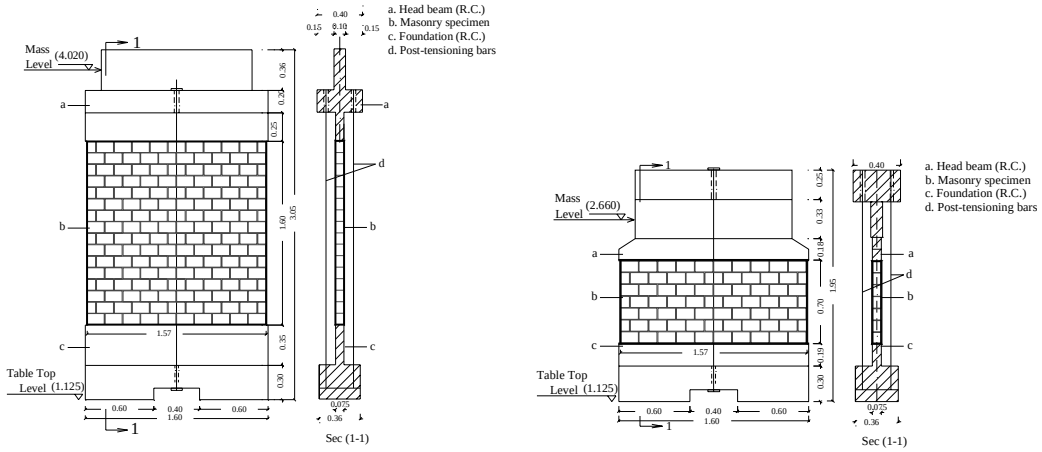

(a) (b)

Figure 1 Specimens dimensions in meter, (a) squat and (b) slender

Table 1: FRP used in the experimental program

Commercial name	FRP [Fiber]	$Warp_W$ [g/m^2]	$Weft_W$ [g/m^2]	f_t [MPa]	E [GPa]	ε [%]
SikaWrap-400A 0/90	Aramid	205	205	2880	100	2.8
SikaWrap-300G 0/90	Glass	145	145	2400	70	3.0
MeC Grid G4000	Glass	139	119	3450	72	4.0
Sika CarboDur S512	Carbon	93	-	2800*	165**	1.7
Sika CarboDur T1.214	Carbon	26	-	2400*	135**	1.6

$Warp_w$ and $Weft_w$: Weight of fiber in the warp and weft directions respectively
f_t and E: Fibers nominal tensile strength and E-modulus respectively
ε: Ultimate strain
*: Composite tensile strength
**: Composite E-modulus

2.2 Test set-up

The specimens tested on the uni-axial earthquake simulator of the Swiss Federal Institute of Technology in Zurich (ETHZ) (Figure 4), details about the test set-up are available in [7 and 14].

2.3 Loading system

A test specimen was constructed on a concrete footing. After allowing the specimen to cure (from 3-7 days), the cap beam was fixed to the top of the specimen using strong mortar (M20). Superimposed gravity load of approximately 30 kN was simulated using two external post-tensioning bars. This was in addition to 12 kN of self-weight from steel elements at wall top (due to the test set-up), reinforced concrete cap beam, and masonry panel weight. This normal force corresponded to a stress of 0.35 MPa. During testing of specimens L1-WRAP-G-F and L1-WRAP-G-X and due to increase of the wall height consecutive to opening of flexural cracks the post-

tensioning force increased many times; in the next specimens two railcar springs were used with the post-tensioning bars.

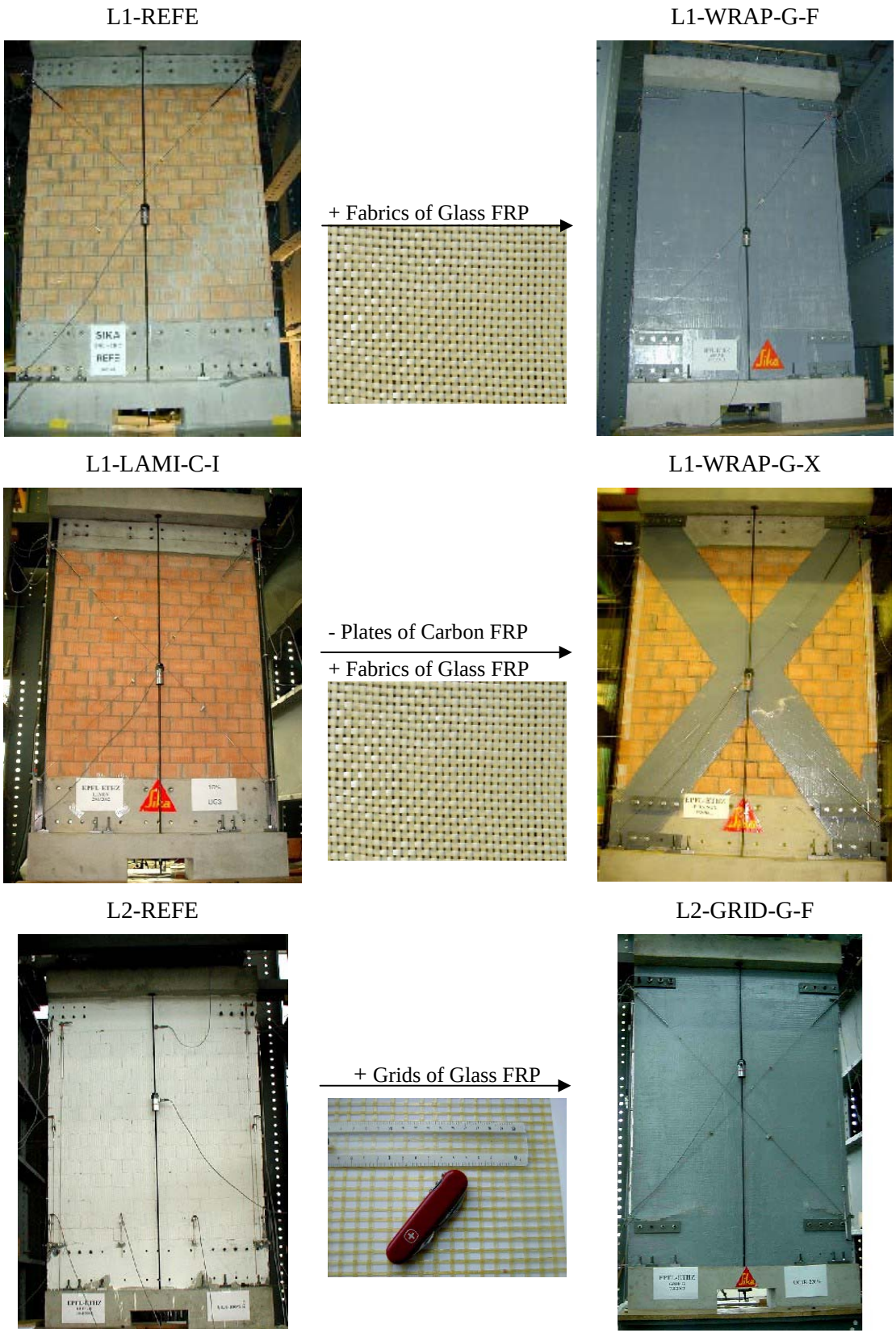

Figure 2 Overview of the tested slender specimens

2.4 Dynamic excitations

The displacement inputs were based on synthetic acceleration time-histories compatible with Eurocode 8 [8] for rock soil type A and with a peak ground acceleration of 1.6 m/s^2 (Figure 5). The specimens were subjected to acceleration histories of increasing intensity until failure occurred. The applied increment was usually 10% of acceleration.

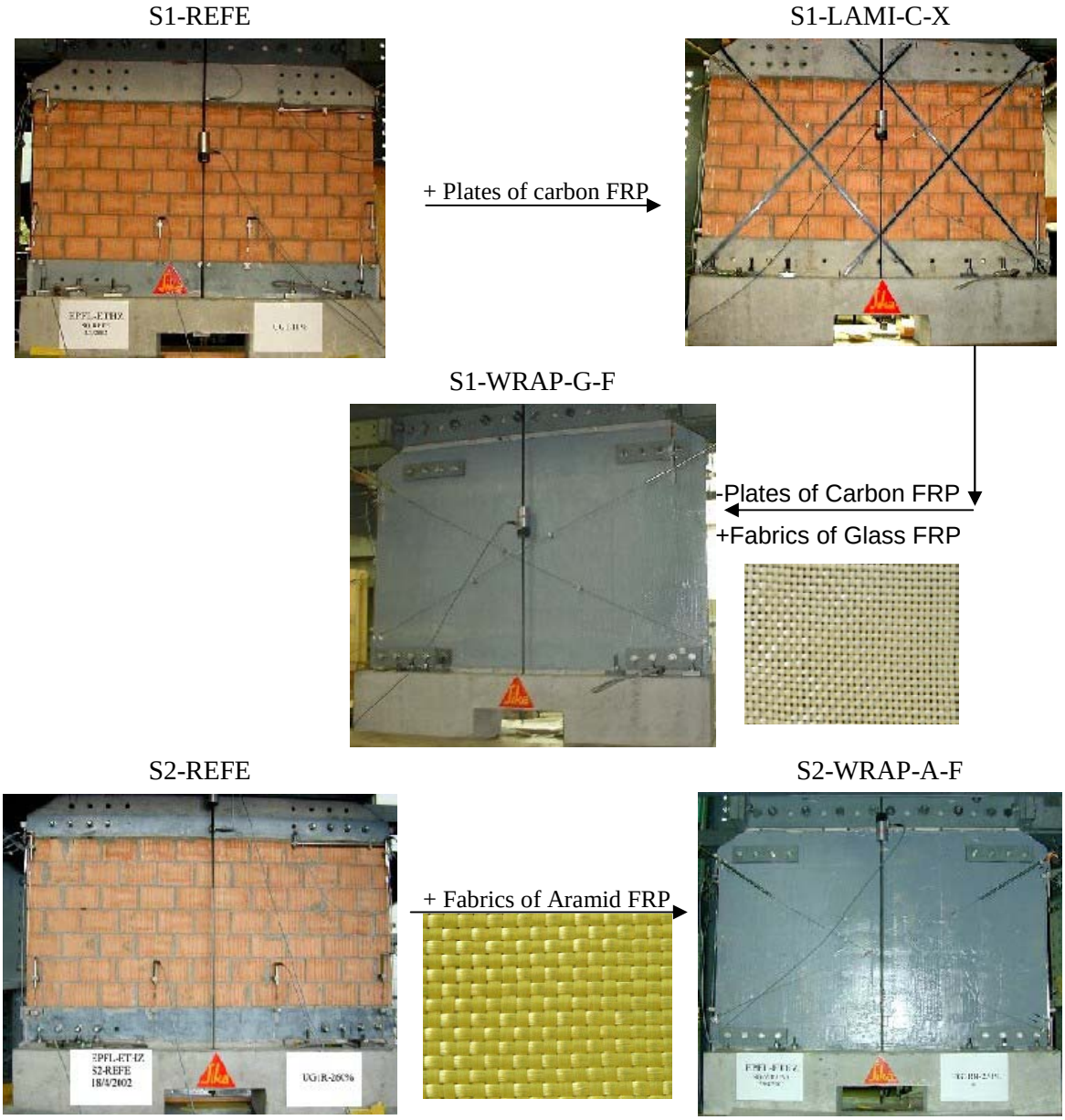

Figure 3 Overview of the tested squat specimens

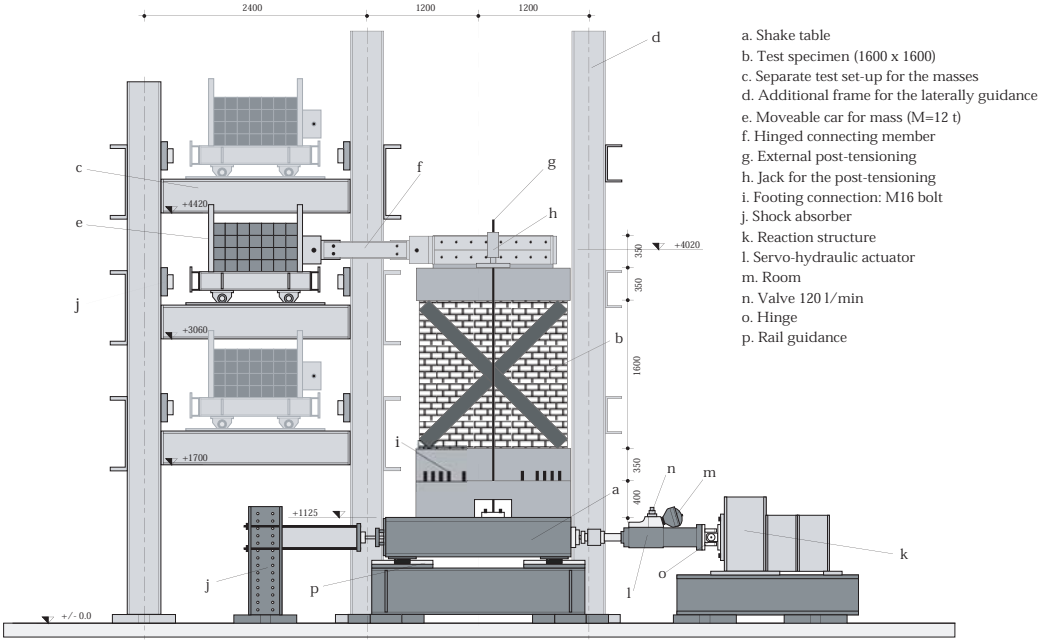

Figure 4 Test Set-up

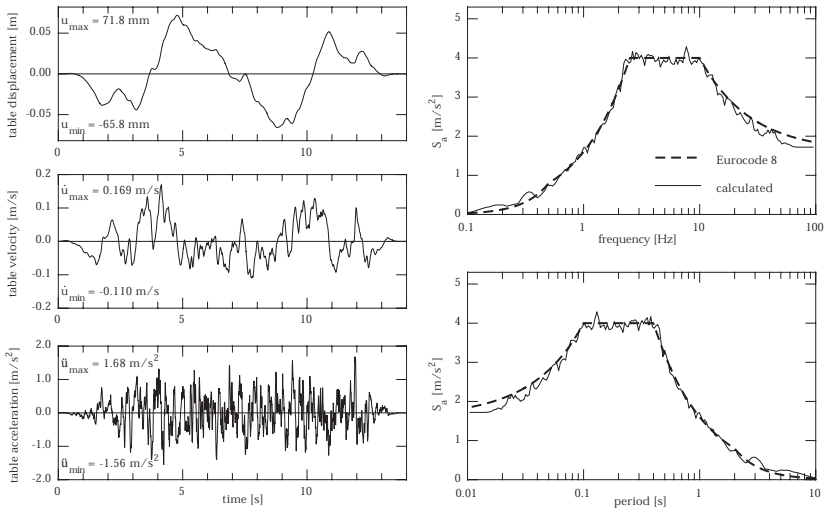

Figure 5 UG1, Eurocode 8 for rock soils type A, spectrum-compatible synthetic earthquake.

3 EXPERIMENTAL RESULTS

3.1 Lateral resistance

All the strengthening materials increased the lateral resistance by a factor ranged from 1.5 to 2.9. Different failure modes were happened during the test; Figure 6 shows the test specimens at the test end. For slender specimens, the full face strengthened specimens (L1-WRAP-G-F and L2-GRID-G-F) developed a rocking mode with masonry crushing at toe and fiber rupture at heal (Figure 7). Under a constant normal force of 57 kN, the strengthening enhanced the lateral resistance by a factor of 2.6 for fabric and 2.9 for grid. A superposition of the hysteresis loops of a reference slender specimen (L2-REFE) and the strengthened specimen L2-GRID-G-F is presented in Figure 8. For L1-WRAP-G-F and at the test end, the normal force tripled (due to increments of wall height as a result of opening of flexural cracks and due to the absence of the railcar springs); this increment in the normal force had insignificant effect on specimen lateral resistance. Nevertheless, the lateral resistance of the reference specimen (L1-REFE) approximately tripled

when the normal force tripled. As a consequence, the enhancement in the lateral resistance in case of high normal force reduced to 1.9 times the original resistance. For squat specimens, the lateral resistances of the full face strengthened specimens (S1-WRAP-G-F and S2-WRAP-G-F) were higher than the machine capacity. At the tests' end, there were no significant signs of failure; in addition, the upgrading enhanced the lateral resistance of the specimens by a factor of 2.6.

Specimens that strengthened with diagonal shape (X) (L1-WRAP-G-X and S1-LAMI-C-X) were less successful. The behaviors of both specimens could be affected by the previous tests which carried out on the specimens before strengthening: before strengthening, L1-WRAP-G-X was tested as L1-LAMI-C-I and S1-LAMI-C-X was tested as S1-REFE. These testes developed several cracks in both specimens. So, the strengthening could be considered as strengthening of URM wall that have been severely damage during a recent real earthquake event. For L1-WRAP-G-X and at failure, the FRP failed at the specimen mid-height due to shear and flexural cracks, which had developed first through mortar joints. For S1-LAMI-C-X and during the test, one plate failed due to anchorage failure at foundation level since no steel plates (which were used in the other specimens to prevent anchorage failure) were used in this specimen. Both strengthening configurations enhanced the lateral resistance by a factor of 1.5 for L1-WRAP-G-X and 1.3 for S1-LAMI-C-X.

3.2 Lateral drift

The ultimate lateral drifts of strengthened specimens were dependent on the aspect ratio and mostly independent on the reinforcement ratio (ρ). For slender specimens (L1-WRAP-G-F, L2-GRID-G-F, and L1-WRAP-G-X) the ultimate drifts were approximately 1%. As an example Figure 9 presents envelope of the hysteresis loops of all the test runs of specimen L2-GRID-G-F; the peak lateral force values are normalized by 128.7 kN, the weights sum of the 12-ton mass, the head beam, half of the masonry panel, and the other test set-up steel elements at specimen top. The envelope clearly shows that approximately 80% of the drift was attributed to specimen rocking. For squat (short) specimens (S1-WRAP-G-F, S2-WRAP-A-F, and S1-LAMI-C-X), it is difficult to prove that the ultimate lateral drifts of strengthened specimens were dependent on the aspect ratio and mostly independent on the reinforcement ratio (ρ) since the specimens (S1-WRAP-G-F, S2-WRAP-A-F) did not reach its ultimate state due to the test set-up capacity. However, the measured maximum drift for the squat upgraded specimens ranged from 0.1% to 0.5%.

3.3 Maximum strains at failure

Recently, several researchers proved that, during testing reinforced concrete beams, the FRP strain at failure is many times lower than its nominal ultimate strains. This phenomenon has been reported for reinforced concrete beams that have been tested in shear ([11] and [16]) as well as in bending [4]; moreover; this phenomenon was presented [12] for URM walls that had been upgraded using GFRP and tested for out-of-plane failure. All these researchers proposed an empirical efficiency factor for FRP; this efficiency factor is inversely proportional to FRP area and Young's modulus. In order to investigate this phenomenon for the tested specimens, the maximum strains, calculated based on the measured deformations using the linear variable displacement (LVD) transducers, at the masonry and strengthened faces of the failed test specimens are examined. The results show that just before failure, the maximum vertical strain for the GFRP fabrics was 1.2% (the nominal ultimate strain for grid fiber is 3%), while for GFRP grids was 2.5% (the nominal ultimate strain for grid fiber is 4%). For the other upgrading materials, no strains at failure were recorded since the FRP did not fail in tension (either debonding and anchorage or no failure at all).

3.4 Specimens asymmetry

As mentioned earlier all the test specimens were strengthened on one side only. As shown by other researchers [3 and 15] this system did not result in any asymmetry in deformations, which may result in more complicated failure mechanism. In order to evaluate this issue for the tested specimens, a comparison between the vertical strains, calculated based on measured displacements using LVD transducers, on the masonry face "bare face" and the strengthened face was carried out. The comparison shows the following:

- For slender specimens, the upgraded system succeeds in producing complete symmetric response in case of tension while there was a little asymmetry in case of compression. The strains indicate that the asymmetry increased by increasing the earthquake intensity, the rate of increase in the asymmetry during compression is many times larger than tension. The maximum asymmetry in tension was recorded during testing L2-GRID-G-F; the average vertical strain along the masonry face was approximately 118% of the average vertical strain along the FRP face. In compression, the maximum asymmetry was recorded during testing L1-WRAP-G-F; the average vertical strain along the masonry face was approximately 50% of the average strain along the FRP face.
- For squat specimens, the upgraded system did not success in producing symmetric response. The maximum asymmetry in tension was recorded during testing S1-WRAP-G-F; the average vertical strain along the masonry face was approximately 290% of the average vertical strain along the FRP face. In compression, the maximum asymmetry was recorded during testing S2-WRAP-A-F; the average vertical strain along the masonry face was approximately 56% of the average strain along the FRP face.

3.5 Anchorage and delamination

As mentioned earlier, the study of the anchorage system was out of the scope of this research; hence, the anchorage failure was prevented by using steel plates at the FRP ends; the steel plates were used in all specimens except in the beginning of testing specimen S1-LAMI-C-X. In all specimens, except S1-LAMI-C-X, this technique prevented the anchorage failure.

Delamination is an important event, since it could be either a raison for stiffness degradation or early sign of failure. The stiffness degradation due to delamination was reported by others [6] for out-of-plane failure of URM-WUC. In order to examine the effect of the strengthening material characteristics on delamination and hence on a specimen behavior, the lateral resistances from each test run were plotted versus the earthquake real intensity. As an example, Figure 11 compares the behavior of specimens L1-WRAP-G-F and L2-GRID-G-F both of them strengthened using a one side full face glass fiber but with different characteristics. The figure shows that, the behavior of both specimens can be described through two phases: before and after delamination. The first phase (before delamination), by increasing the earthquake real intensity (acceleration) the lateral resistance of both specimens increased linearly, approximately, in an identical way. In this phase no large variations in the post-tensioning forces, in both specimens, were recorded. The second phase started with delamination; after delamination both specimens behaved in a nonlinear way; there was nonlinear increase in the lateral resistance with increasing earthquake real intensity. This nonlinear behavior was combined with high increase in the post-tensioning force in case of L1-WRAP-G-F (note that no railcar springs were used). In case of L2-GRID-G-F, the post-tensioning force remained approximately constant till 232% of real earthquake intensity; after rupture of the grids, the real earthquake intensity decreased while the corresponding post-tensioning force increased many times. Moreover, examination of FRP strains at first delamination for all the tested specimens shows the following:

- The lateral resistance at first delamination (Fd) is proportional to the fiber ultimate strength and inverse proportional to the reinforcement ratio.
- Qualitatively Fd is influenced by three factors: the aspect ratio, the FRP product and material type, and the upgrading configuration.
- The glass fiber fabrics delaminated at average tensile strains approximately ranged from 0.06% to 0.32%, depends on the reinforcement ratio.
- The glass fiber grids delaminated at average vertical tensile strains approximately 0.09%.
- The thermoplastic plates of CFRP “Sika CarboDur T” failed due to anchorage at average tensile strains of 0.4%; after reparation using fast epoxy, it delaminated at average tensile strain of 0.5%.
- For all specimens, that had delaminated, the average vertical compression strains along the masonry panel, at delamination, was approximately 0.04% independent on the reinforcement ratio or product.

3.6 Natural frequencies

Fast Fourier transforms (FFTs) were computed from the relative horizontal acceleration response time-histories of the mass collected during the dynamic test runs. The relative horizontal acceleration of the mass is the difference between the absolute horizontal acceleration measured on the mass and the table acceleration. The oscillation of the mass reflects the wall behavior therefore the fundamental frequency was defined as the location of the peak Fourier amplitude between 1 Hz and 5 Hz for each test run. The lower bound, of this range, avoided low frequency disturbances appearing from measurements and numerical imprecision. The upper bound , of this range, avoided high frequency disturbances appearing from hydraulic jack. As shown in (Figure 10) several Fourier amplitude peaks at similar locations appeared in the investigated frequency. From a test run to the following test run, the relative amplitudes of the peaks rather than their location were modified. This feature is a characteristic of non-linear behavior. As a consequence, the fundamental frequency did not change gradually with increasing the test runs but rather dropped suddenly from a peak to another after staying constant at the same peak for several test runs.

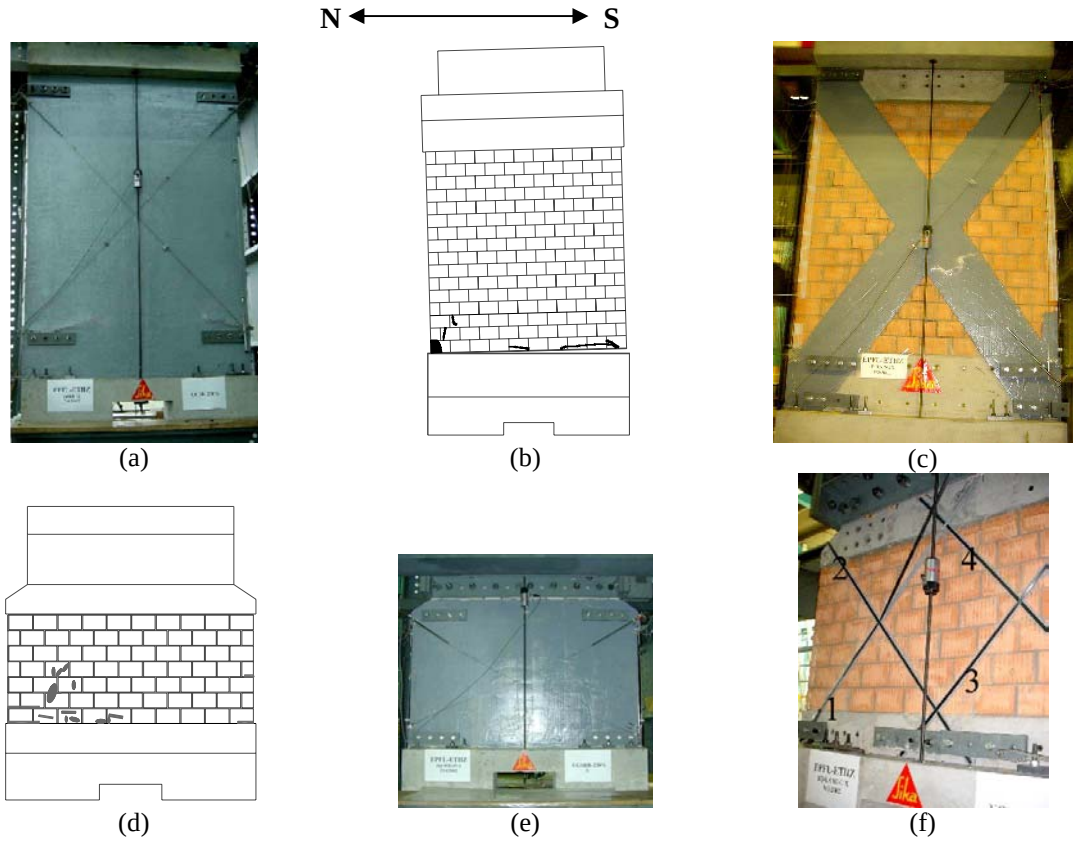

Figure 6 Failure modes of specimens (a) L2-GRID-G-F, (b) L1-WRAP-G-F, (c) L1-WRAP-G-X, (d) S1-WRAP-G-F, (e) S2-WRAP-A-F, and (f) S1-LAMI-C-X

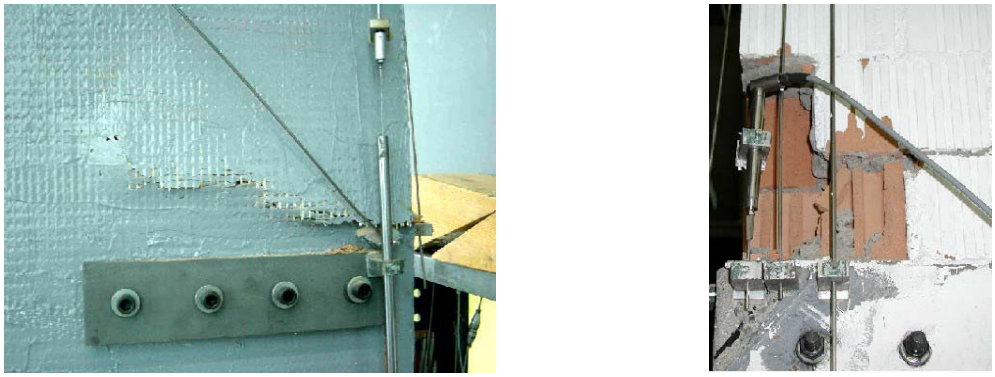

(a) (b)

Figure 7 L2-GRID-G-F at the test end (a) grid rupture in the bottom western south side, (b) masonry failure in the bottom eastern south side

4 Conclusion

Five half-scale URM walls were built using half scale brick units. These five walls were dynamically tested as reference specimens. Then, these reference specimens were upgraded using composites and retested. As a consequence, a total of eleven specimens were tested on the earthquake simulator of ETHZ. This research has investigated the following parameters:

- the aspect ratio: slender (aspect ratio of 1.4) and squat (aspect ratio of 0.7)
- the fiber type: aramid, glass, and carbon fiber
- the upgrading configurations: diagonal shape (X) and wrapping
- the fiber structures: plates, fabrics, and grids
- the mortar compressive strength: weak (M2.5) and strong (M9).

The dynamic experimental testing of six URM-WUC specimens, led to the following findings:

- The upgrading materials increased the specimens' lateral resistances by a factor of 1.4 to 2.9 compared to the reference (URM) specimens. Expectedly, the increase ratio is higher for lower normal force: the lateral resistance of the reference specimen increases, approximately in a linear fashion, by increasing the normal force; nevertheless, the increase in the normal force has little effect on the resistance of the upgraded specimens.
- The enhancement in the ultimate drift for the slender upgraded specimens was small, reaching up to 1.2. Furthermore, the ultimate drifts were independent on the reinforcement ratio and reinforcement type (grid or fabric); however, the ultimate drifts were dependent on the aspect ratio and the upgrading configuration.
- Within the test conditions, upgrading on one side appears to produce good behavior. No out-of-plane or uneven response of the specimens was observed. Small asymmetries in the transducers were recorded in the case of squat specimens. However, further investigations are required for squat specimens in the ultimate range.
- In some specimens there was debonding of the fibers/grids in the form of white spots. This debonding occurred at different lateral load levels, which ranged from 50% to 80% of the ultimate load resistance. The lateral resistance at first delamination is strongly dependent on the reinforcement ratio and specimen aspect ratio as well as the fiber characteristics.
- The fabric prevented falling of debris from the wall after failure; thus, preventing possible injuries to occupants in the vicinity of the wall in the event of an earthquake in a real case.
- In general, the bi-directional surface type materials (fabrics and grids) applied on the entire surface of the wall (and correctly anchored) can help postpone the three classic failure modes of masonry walls: rocking ("flexural failure"), step cracking and sliding ("shear failures"). In other terms, they are robust: even if the engineer is not sure of the expected failure mode

before/after retrofit, the retrofit can help. Additionally, in some situations, they will postpone in-plane collapse by "keeping the bricks together" under large seismic deformations.

- Carbon plates or fabric strips used in a diagonal pattern (X or XX) was less successful. It was used in the upgrading of two specimens; in both cases, "premature" failure developed (anchorage once and shear-flexure another). In both cases, the retrofit pattern and reinforcement ratio could have been improved to prevent the premature failure; however, the tests indicate that these retrofits are less robust and less redundant.

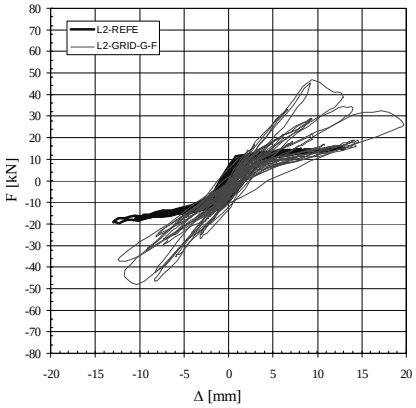

Figure 8 Superposition of the hysteretic loops of reference specimen (L2-REFE) and upgraded specimen (L2-GRID-G-F)

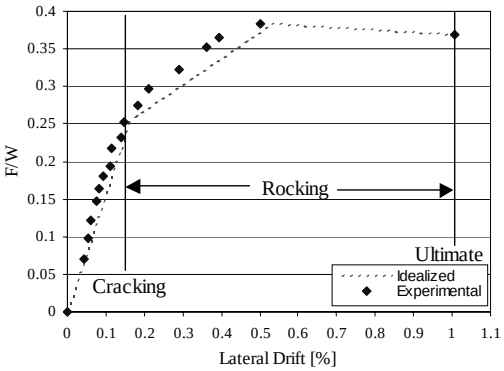

Figure 9 Normalized peak lateral force vs. specimen drift for L2-GRID-G-F

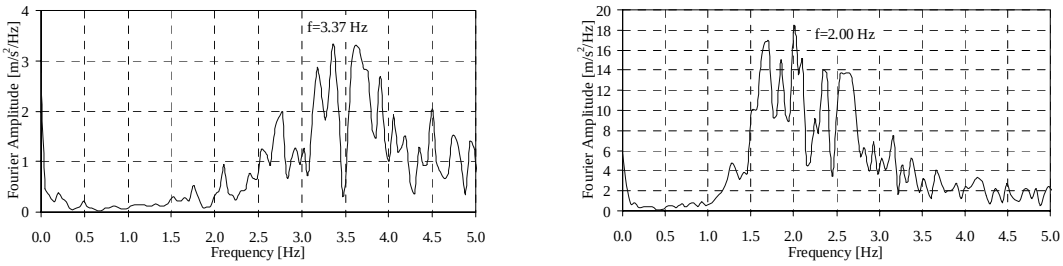

(a) (b)

Figure 10 Fourier amplitude spectra for relative mass accelerations of specimen L2-GRID-G-F, (a) before cracking, and (b) at the test end

References

[1] *Abrams, D. P., and Lynch, J. M. (2001). "Flexural behavior of retrofitted masonry piers." KEERC-MAE Joint Sem. on Risk Mitigation for Regions of Moderate Seismicity, Illinois.*

[2] *Albert, M. L., Elwi, A. E., and Cheng, J. J. R. (2001). "Strengthening of unreinforced masonry walls using FRPs." J. Comp. for Constr., ASCE, 5 (2).*

[3] Al-Chaar, G. K., and Hasan, H. (1999). "Masonry bearing and shear walls retrofitted with overlay composite material." U.S. Army, Corps of Engineers, Champaign, *Technical Report 98/86*.

[4] Bonacci F. J.; Maalej, M (2001), "Behavioral Trends of RC Beams Strengthened with Externally Bonded FRP" *J. Comp. for Constr.,* ASCE, 5(2).

[5] El-Dakhakhani, W. W. (2002). "Experimental and analytical seismic evaluation of concrete masonry-infilled steel frames retrofitted using GFRP laminates." PhD dissertation, college of Engineering, Drexel University, USA.

[6] *Ehsani, M. R., Saadatmanesh, H., Velazquez-Dimas, J. I. (1999). "Behavior of retrofitted URM walls under simulated earthquake loading." J. Comp. for Constr., ASCE, 3(3).*

[7] *ElGawady, M. A., Lestuzzi, P., Badoux, M. (2003): Dynamic tests on URM walls before and after upgrading with composites http://imacwww.epfl.ch/imac/Team/Elgwady/Publication/ EPFL_URM_WUC.pdf*

[8] *Eurocode 8 (1994). "Design provisions for earthquake resistance of structures." Comite Euro-International du Béton, Lausanne, Switzerland.*

[9] *Hamilton III, H. R., and Dolan, C. W, (2001), "Flexural capacity of glass FRP strengthened concrete masonry walls." J. Comp. for Constr., ASCE, 5(3).*

[10] *Holberg, M., and Hamilton, R., (2002). "Strengthening URM with GFRP composites and ductile connections." Earth. Spec., 18(1).*

[11] Khalifa, A., Gold, W., Nanni, A., and Abdel Aziz, I. (1998). "Contribution of externally bonded FRP to shear capacity of RC flexural members." *J. Comp. for Constr.,* ASCE, 2(4).

[12] Kuzik, M. D., Elwi, A. E, and Cheng, J. J. R. (2003). "Cyclic flexural tests of masonry walls reinforced with glass fiber reinforced polymer sheets." *J. Comp. for Constr.,* ASCE, 7(1).

[13] Lang, K. (2002). "Seismic vulnerability of existing buildings." PhD dissertation, Institute of Structural Engineering, Department of Civil, Environmental and Geomatics Engineering, Swiss Federal Institute of Technology, Zurich, Switzerland.

[14] *Lestuzzi, P., Wenk, T., and Bachmann, H. (1999). "Dynamic tests of RC structural walls on the ETH earthquake simulator." Report No. 240, IBK, Department of Civil, Environmental and Geomatics Engineering, Swiss Federal Institute of Technology, Zurich, Switzerland.*

[15] *Schwegler, G., (1994). "Masonry construction strengthened with fiber composites in seismically endangered zones." 10th ECEE, Vienna.*

[16] Triantafillou, T. C. (1998). "Strengthening of masonry structures using epoxy-bonded FRP laminates." *J. Comp. for Constr.,* ASCE, 2(2).

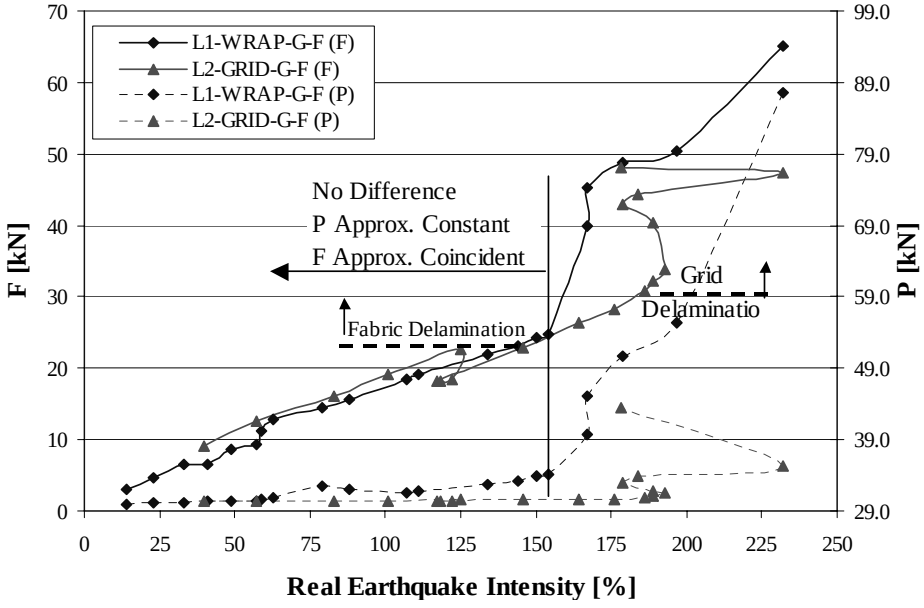

Figure 11 Comparison between measured lateral resistances (F) and post-tensioning forces (P) for slender reinforced specimens L1-WRAP-G-F and L2-GRID-G-F